Matter and Radiation at Extremes | LETTER | scitation.org/journal/mre

Injection induced by coaxial laser interference in laser wakefield accelerators

Cite as: Matter Radiat. Extremes 7, 054001 (2022); doi: 10.1063/5.0101098
Submitted: 29 May 2022 • Accepted: 31 July 2022 •
Published Online: 1 September 2022

Jia Wang,[1,2] Ming Zeng,[1,2,a)] Dazhang Li,[1,2,a)] Xiaoning Wang,[1,2] Wei Lu,[3] and Jie Gao[1,2]

AFFILIATIONS

[1] Institute of High Energy Physics, Chinese Academy of Sciences, Beijing 100049, China
[2] University of Chinese Academy of Sciences, Beijing 100049, China
[3] Department of Engineering Physics, Tsinghua University, Beijing 100084, China

[a)] **Authors to whom correspondence should be addressed:** zengming@ihep.ac.cn and lidz@ihep.ac.cn

ABSTRACT

We propose a new injection scheme that can generate electron beams with simultaneously a few permille energy spread, submillimeter milliradian emittance, and more than a 100 pC charge in laser wakefield accelerators. In this scheme, a relatively loosely focused laser pulse drives the plasma wakefield, and a tightly focused laser pulse with similar intensity triggers an interference ring pattern that creates onion-like multisheaths in the plasma wakefield. Owing to the change in wavefront curvature after the focal position of the tightly focused laser, the innermost sheath of the wakefield expands, which slows down the effective phase velocity of the wakefield and triggers injection of plasma electrons. Both quasicylindrical and fully three-dimensional particle-in-cell simulations confirm the generation of beams with the above mentioned properties.

There has been tremendous progress in laser wakefield accelerators (LWFAs) in recent decades, and they have become one of the most important candidates for the next generation of accelerator-based light sources and colliders.[1–7] The present energy record in LWFA experiments is 7.8 GeV,[8,9] and the typical energy spread is in the range of a few percent, with the lowest reported value being slightly below 1%, with beam charges of tens of picocoulombs.[10–12] However, for challenging applications such as plasma-based colliders and free-electron lasers, orders of magnitude better beam qualities are required, and need to be achieved simultaneously, and this has motivated an ongoing search for methods of generating high-quality beams.[13–16]

Among these methods, all-optical injection schemes are very attractive owing to their simple setups and their potential for precise controllability.[17–19] Experimental demonstrations of these schemes and modified versions typically produce electron beams with energy spread >1% and charges of tens of picocoulombs.[20–25] Further optimization of these schemes, based on particle-in-cell (PIC) simulations,[26–30] and optimizations of other injection schemes relying on assistant lasers such as plasma torches[31] and Trojan Horse injection,[32–34] as well as of methods that rely on higher laser modes,[35] have suggested that better beam qualities are attainable. However, none of these studies has produced a beam with simultaneously small energy spread of a few permille, small emittance (<0.5 mm mrad), and large amount of charge (>100 pC).

In this work, we propose a novel all-optical injection scheme that can generate high-quality electron beams with parameters beyond the above-mentioned values, by utilizing the interference of two coaxial laser pulses. In this scheme, a driver laser pulse, containing the majority of the total energy, is relatively loosely focused, with its Rayleigh range covering the injection region, while a trigger pulse, containing only a small portion of the total energy, is tightly focused shortly before the injection region, as illustrated in Fig. 1(a). Because of the different wavefront curvatures of the two lasers, interference rings are formed in the cross-section of the lasers, pinching the plasma electrons in the traps of their ponderomotive force.[36] As a result, onion-like multiple subcavities are formed in the plasma wake, as shown in Fig. 1(b). With the propagation of the two lasers, the innermost subcavity expands, which slows down the effective phase velocity of the wake. Such an injection process is similar to density down-ramp injection. The one-to-one mapping between the injection phase and the initial phase greatly limits

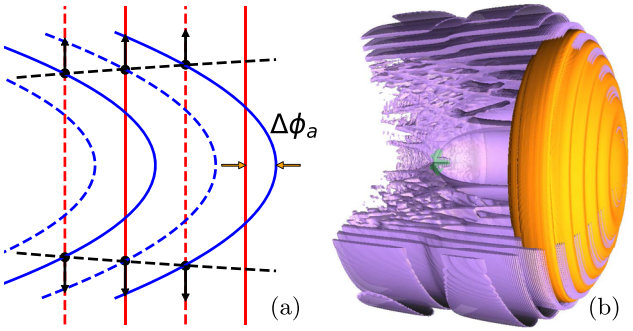

FIG. 1. Illustration of the coaxial interference of the two laser pulses (a), which creates an onion-like plasma wake (b) in the proposed injection scheme. (a) The driver laser (red lines) is relatively loosely focused and the trigger laser (blue lines) is tightly focused, with the peak wavefront illustrated by solid lines and the valley wavefront by dashed lines. Both lasers move to the right. The axial phase difference of the two lasers is $\Delta\phi_a$. The intersections of different types of lines, marked as black dots, are destructive points (rings in cylindrical geometry). The lines connecting the black dots become the subcavity sheath of the wakefield. The black arrows indicate the direction of motion of the sheath. (b) Isosurface plot of the laser (orange), plasma (violet), and injected electron beam (cyan) from a 3D simulation. A quarter of the plasma is cut away to show the interior.

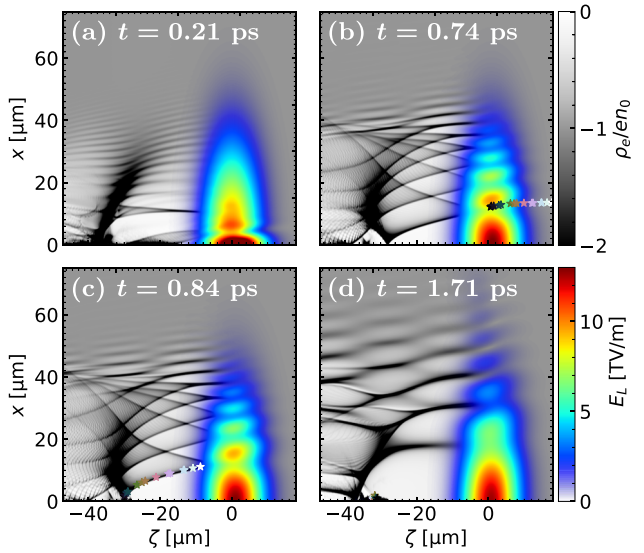

FIG. 2. Simulation of the proposed injection scheme. A driver laser with peak power 227.13 TW is focused to a waist of $w_{00} = 30$ μm, and a trigger laser with peak power 1.88 TW is focused to a waist of $w_{01} = 2$ μm. In the plots, the profile of the summation of the electric fields of both lasers is shown as E_L by omitting the oscillation in the laser frequency scale. The snapshots show the innermost subcavity: (a) this subcavity is not big enough to sustain an injection; (b) it is big enough, and injection starts; (c) it is expanding, and injection continues; (d) it reaches its maximum size, and injection stops. A sample of injected electrons are marked as stars.

phase mixing and thus guarantees a small slice energy spread, and the defocusing force near the rear of the bubble kicks the electron trajectories from larger ellipses to smaller ones in the transverse space–momentum phase space, ensuring a small emittance of the trapped beam.[37,38] The small slice energy spread is transformed to a small energy spread of the entire beam by the self-dechirping effect, which is to be discussed later. The injection length is a few hundred micrometers, which is significantly longer than those in previous all-optical injection studies, allowing large amount of beam charge.

Owing to its close-to-cylindrical feature, this scheme is suitable for simulation using the spectral quasicylindrical algorithm, which decomposes the Maxwell equations in k space through a Hankel–Fourier transform with only a few azimuthal modes and is more computationally efficient than a fully 3D algorithm.[39] An example of a simulation using the code WarpX with the spectral quasicylindrical algorithm and the PSATD (Pseudo-Spectral Analytical Time Domain) solver[40] is shown in Fig. 2. In the plots, the longitudinal coordinate is transformed to the comoving frame $\zeta = z - ct$, where z is the longitudinal position, with its zero point at the beginning of the flattop of the plasma density profile, c is the speed of light in vacuum, and t is the time, with its zero point at the instant when the driver laser center reaches $z = 0$. In this simulation, the unperturbed plasma density profile has a linear up-ramp from $z = -50$ μm to 0 and a flattop from $z = 0$ to $+\infty$, with the density of the flattop $n_0 = 1 \times 10^{18}$ cm^{-3}. The driver laser has a peak power of 227.13 TW and is focused at $z = z_{f0} = 450$ μm, with a focal waist of $w_{00} = 30$ μm. The trigger laser has a peak power of 1.88 TW and is focused at $z = z_{f1} = 40$ μm, with a focal waist of $w_{01} = 2$ μm. Both lasers have wavelength $\lambda = 0.8$ μm and pulse duration of 25 fs and are linearly polarized in the y direction (perpendicular to the paper), but the trigger laser is 3.75λ ahead of the driver laser. The longitudinal size of the simulation box is 65 μm, with 4096 cells, the transverse size is 500 μm, with 1024 cells, the number of azimuthal modes is 2, and the time step interval is dz/c, where dz is the longitudinal grid size. The number of macroparticles per cell is 192 in the injection region and 24 elsewhere. Owing to the interference of the two lasers, rings with ponderomotive traps are formed, creating subcavities in the plasma wake. The expansion of the innermost subcavity sharply slows down the effective phase velocity of the wakefield from $t = 0.6$ to 1.7 ps, as shown in Fig. 3(a), and thus injection of background plasma electrons occurs, forming a beam with ~0.5 MeV slice energy spread. The longitudinal electric field exerts positive and negative chirping on the injected beam respectively before and after $t = 18$ ps, where the blowout regime is transformed to a partial-blowout regime, as shown in Figs. 3(b) and 3(c), owing to the pump-depletion effect of the driver pulse.[41] The energy spread has two minima before and after the self-dechirping point, as shown in Figs. 3(d)–3(g). It can be seen that a 170 pC electron beam with energy spread no more than 0.4% and emittance no more than 0.5 mm mrad is generated. It is worth noting that the two local minima of the energy spread do not persist for other acceleration distances, owing to the non-uniform acceleration field.

A full 3D simulation with the same grid size and parameters as above has also been performed (but only until injection has finished, owing to limited computational resources). The injected beam has a normalized emittance of 0.14 mm mrad in both transverse directions, a charge of 150 pC, and a slice energy spread of ~0.5 MeV,

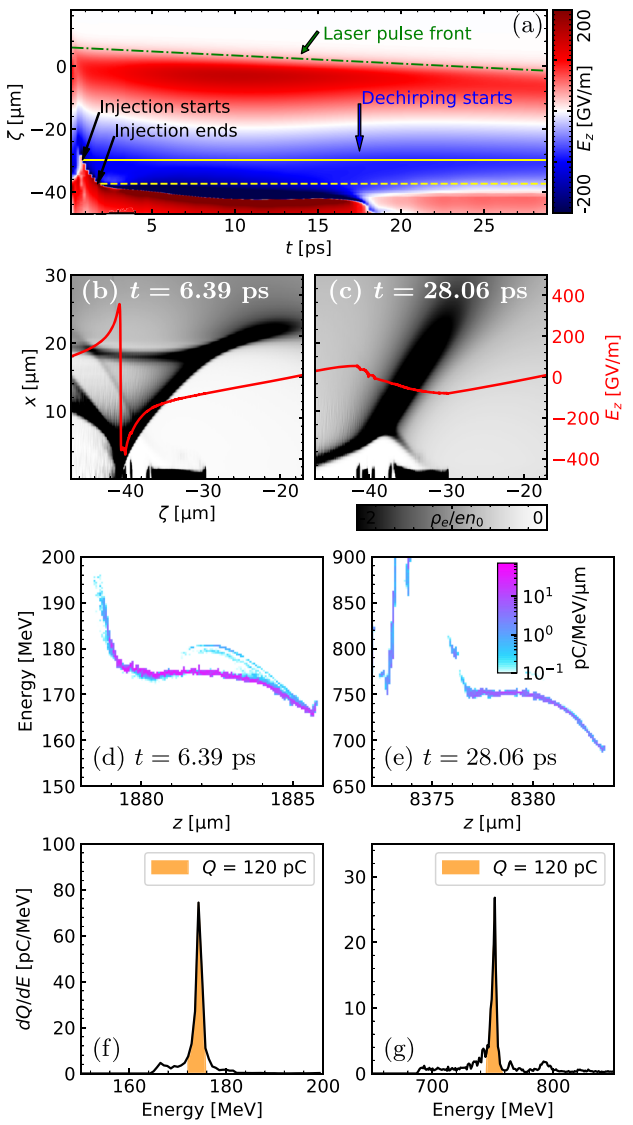

FIG. 3. Plots showing injection, self-dechirping, and beam quality. (a) Evolution of the axial longitudinal electric field E_z. The contour of the laser pulse front is shown as a green dash-dotted line and those of the head and tail of the injected electron beam as yellow solid and dashed lines, respectively. (b) and (c) Snapshots at $t = 6.39$ and 28.06 ps (before and after self-dechirping). The phase spaces and energy spectra of the injected electron beam at these two instants of time are shown in (d) and (f) and in (e) and (g), respectively. The energy spread, the charge within threefold energy spread (colored areas), and the normalized emittance in the (x, y) directions are (f) 0.4%, 120 pC, (0.15, 0.05) mm mrad and (g) 0.34%, 120 pC, (0.25, 0.5) mm mrad. The total charge of this beam is 170 pC which does not change with time after injection has finished.

which confirms the validity of the quasicylindrical simulation. This simulation at $t = 1$ ps is plotted in Fig. 1(b).

To explain the physics of the multisheath creation and injection, we write down the expression for the electric field of a Gaussian laser pulse in vacuum:

$$E(r,z,t) = E_0 \frac{w_0}{w(z)} T(z-ct) \exp\left[-\frac{r^2}{w^2(z)} + i\phi\right], \tag{1}$$

where E_0 is the peak electric field strength at the focus, w_0 is the laser waist radius, $r = \sqrt{x^2+y^2}$ is the transverse position, $w(z) = w_0\sqrt{1+(z-z_f)^2/z_R^2}$ is the laser radius, z_f is the focal position, $z_R = \pi w_0^2/\lambda$ is the Rayleigh length, $T(z-ct) = \exp[-(z-ct-z_0)^2/(c\tau)^2]$ is the temporal profile of the pulse, z_0 is the pulse center at $t = 0$, τ is the pulse duration,

$$\phi = -k\left[\frac{r^2}{2R(z)} + z - ct - z_0\right] + \phi_{\rm CEP} + \phi_{\rm G} \tag{2}$$

is the phase, $k = 2\pi/\lambda$ is the wavenumber, $\phi_{\rm CEP}$ is the carrier envelope phase (CPE),

$$R(z) = z - z_f + \frac{z_R^2}{z - z_f} \tag{3}$$

is the radius of the wavefront curvature, and

$$\phi_{\rm G} = \arctan\left(\frac{z-z_f}{z_R}\right) \tag{4}$$

is the Gouy phase. We neglect the plasma reaction to the laser pulses, because the interference region is short compared with the self-focusing length,[42] and the phase velocity changes due to the plasma reaction are the same for the two lasers. We use extra subscripts 0 and 1 for the driver and trigger lasers, respectively, and the axial phase difference of the two lasers is then

$$\Delta\phi_a \equiv \phi_1|_{r=0} - \phi_0|_{r=0} = \Delta\phi_{-\infty} + \Delta\phi_{\rm G}, \tag{5}$$

where $\Delta\phi_{-\infty} = k\Delta z_0 + \Delta\phi_{\rm CEP}$ is the phase difference far before focus, $\Delta z_0 = z_{01} - z_{00}$ is the difference of the centers of the two pulses, $\Delta\phi_{\rm CEP} = \phi_{\rm CEP1} - \phi_{\rm CEP0}$ is the difference of the carrier envelope phases, and $\Delta\phi_{\rm G} = \phi_{\rm G1} - \phi_{\rm G0}$. The phase difference for arbitrary r can be written as

$$\begin{aligned}\Delta\phi = \phi_1 - \phi_0 &= \frac{kr^2}{2}\left(\frac{1}{R_0} - \frac{1}{R_1}\right) + \Delta\phi_a \\ &\approx -\frac{kr^2}{2}\frac{1}{R_1} + \Delta\phi_a,\end{aligned} \tag{6}$$

where only $z > z_{f1}$ (and thus $R_1 > 0$) is considered, and the approximation is taken because $|R_0| \gg R_1$ in the injection region. The destructive inference rings have $\Delta\phi = -(2m+1)\pi$, where m is an integer. These rings are ponderomotive traps, pinching the stream of background electrons and forming subcavity sheaths. Thus, the radii of the subcavities are

$$r_c = \sqrt{\frac{2R_1}{k}[(2m+1)\pi + \Delta\phi_a]}. \tag{7}$$

Without loss of generality, we shift $\Delta\phi_a$ to the range $(-\pi, \pi]$ by adding a multiple of 2π. Then, m should be a non-negative integer, and the radius of the innermost subcavity is

$$r_c^* \equiv r_c|_{m=0} = \sqrt{\frac{2R_1}{k}(\pi + \Delta\phi_a)}. \tag{8}$$

On the basis of simulation observations, we assume that the longitudinal extent of the innermost subcavity can be estimated by $L_c \sim 2r_c^*$. Because the front half of the main wakefield bubble has a decelerating electric field, and the subcavity cannot be longer than the main bubble, a necessary (but not sufficient) condition for injection is

$$L_b/2 < L_c < L_b, \tag{9}$$

where L_b is the longitudinal extent of the main bubble. This implies $|z - z_{f1}| \gg z_{R1}$ and $|z - z_{f0}| \ll z_{R0}$ in the injection region, which lead to $\Delta\phi_G \approx \pi/2$ and $R_1 \approx z - z_{f1}$. Thus, Eq. (8) can be simplified in the injection region as follows:

$$r_c^* \approx \sqrt{\frac{3\pi + 2\Delta\phi_{-\infty}}{k}}\sqrt{z - z_{f1}}, \tag{10}$$

where $\phi_{-\infty}$ is shifted to the range $(-3\pi/2, \pi/2]$ by adding a multiple of 2π. The increasing r_c^* leads to an increasing L_c and a slow-down of the wakefield phase velocity, which triggers injection of electrons from the subcavity sheath.

To investigate the influence of the initial phase difference $\Delta\phi_{-\infty}$, we vary Δz_0 from 3.7 λ to 4.7 λ while keeping $\Delta\phi_{\mathrm{CEP}} = 0$. The theoretical evolution of the peak axial electric field E_p, obtained by adding the electric field of the two lasers using Eq. (1), is shown in Fig. 4(a) as solid lines. The simulation results are plotted as scatter points and show reasonably good agreement with theory. The injected beam charge has a strong correlation with E_p at $z = 150$ μm, which is a typical injection location, as shown in Fig. 4(b). Injection is suppressed if $\Delta\phi_{-\infty} \approx \pi/2$ (thus, $\Delta\phi_a \approx \pi$ with the same assumption as previously, $\Delta\phi_G \approx \pi/2$), because the interference is destructive on axis and the innermost subcavity does not have a clear sheath. It is worth noting that $\Delta z_0 = 3.75$ λ was used for the simulation shown in Figs. 2 and 3, which maximized the injection quantity.

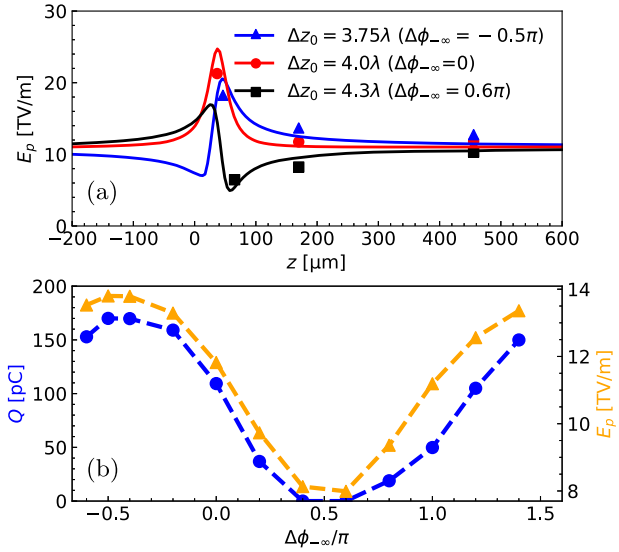

FIG. 4. Dependence of the peak superimposed axial electric field of the two lasers E_p and the injected charge on the initial phase difference of the two lasers $\Delta\phi_{-\infty}$, which is varied by changing Δz_0 while keeping $\Delta\phi_{\mathrm{CEP}} = 0$. (a) E_p vs z for different $\Delta\phi_{-\infty}$ cases. The solid lines represent the theoretical values and the scatter points are from simulations. (b) Beam charge after injection has finished (blue) and E_p at $z = 150$ μm (yellow) vs $\Delta\phi_{-\infty}$ obtained from simulations.

To test the influence of laser pointing jitter, we have also performed one full 3D simulation with the trigger pulse transversely offset by 2 μm, which shows that the emittance of the trapped beam in the offset direction increases to 2 mm mrad, the emittance in the vertical direction and the slice energy spread do not change significantly, and the amount of charge decreases to 115 pC. Thus, this injection scheme is robust under micrometer-scale jitter of the transverse focal position.

In summary, we have proposed a new injection scheme for laser wakefield accelerators that generates electron beams with simultaneously small energy spread, small emittance, and large amount of charge. In this scheme, one laser pulse is relatively loosely focused to drive the plasma wakefield, and another laser is tightly focused in the Rayleigh range of the former. The energy of the latter laser is only a small portion of the former, but the peak intensities are similar owing to their focal spot size difference. Within a certain range, the tightly focused laser has a convex wavefront, while the wavefront of the loosely focused laser is flat. Consequently, interference rings are formed, pinching the background electron stream and creating subcavities in the wakefield. owing to the rapidly varying wavefront curvature of the tightly focused laser, the innermost subcavity expands, slows down the effective phase velocity of the wakefield, and triggers the injection of an electron beam with a few permille energy spread and no more than 0.5 mm mrad emittance. The charge of the injected beam can be modulated by the initial phase difference of the two lasers, with the maximum exceeding 100 pC for a moderate total laser power ~200 TW. This mechanism is sensitive to the phase difference of the two lasers, which can be either time delay or carrier envelope phase (CEP) difference. In practice, the CEP difference can be eliminated by obtaining the two laser beams by splitting one laser beam, and the time delay should be precisely controlled to maximize the injection quantity.

This work is supported by the Research Foundation of the Institute of High Energy Physics, Chinese Academy of Sciences (Grant Nos. E05153U1, E15453U2, Y9545160U2, and Y9291305U2) and the Key Research Program of Frontier Sciences of the Chinese Academy of Sciences (Grant No. QYZDJ-SSW-SLH004).

AUTHOR DECLARATIONS

Conflict of Interest

The authors have no conflicts to disclose.

Author Contributions

Jia Wang: Conceptualization (equal); Data curation (equal); Formal analysis (equal); Investigation (equal); Visualization (equal);

Writing – original draft (equal); Writing – review & editing (supporting). **Ming Zeng**: Conceptualization (equal); Data curation (equal); Formal analysis (equal); Funding acquisition (equal); Investigation (equal); Methodology (lead); Resources (equal); Supervision (equal); Validation (equal); Visualization (equal); Writing – original draft (equal); Writing – review & editing (equal). **Dazhang Li**: Conceptualization (equal); Funding acquisition (equal); Methodology (equal); Project administration (equal); Resources (equal); Supervision (equal); Writing – original draft (equal); Writing – review & editing (equal). **Xiaoning Wang**: Investigation (supporting); Resources (supporting); Writing – review & editing (supporting). **Wei Lu**: Methodology (supporting); Writing – original draft (supporting); Writing – review & editing (lead). **Jie Gao**: Funding acquisition (equal); Project administration (supporting); Supervision (equal); Writing – review & editing (supporting).

DATA AVAILABILITY

The data that support the findings of this study are available upon reasonable request from the authors.

REFERENCES

[1]T. Tajima and J. M. Dawson, "Laser electron accelerator," Phys. Rev. Lett. **43**, 267–270 (1979).

[2]S. P. D. Mangles, C. D. Murphy, Z. Najmudin, A. G. R. Thomas, J. L. Collier, A. E. Dangor, E. J. Divall, P. S. Foster, J. G. Gallacher, C. J. Hooker *et al.*, "Monoenergetic beams of relativistic electrons from intense laser–plasma interactions," Nature **431**, 535–538 (2004).

[3]J. Faure, Y. Glinec, A. Pukhov, S. Kiselev, S. Gordienko, E. Lefebvre, J.-P. Rousseau, F. Burgy, and V. Malka, "A laser–plasma accelerator producing monoenergetic electron beams," Nature **431**, 541–544 (2004).

[4]C. G. R. Geddes, C. Toth, J. Van Tilborg, E. Esarey, C. B. Schroeder, D. Bruhwiler, C. Nieter, J. Cary, and W. P. Leemans, "High-quality electron beams from a laser wakefield accelerator using plasma-channel guiding," Nature **431**, 538–541 (2004).

[5]Y. Ma, J. Hua, D. Liu, Y. He, T. Zhang, J. Chen, F. Yang, X. Ning, Z. Yang, J. Zhang, C.-H. Pai, Y. Gu, and W. Lu, "Region-of-interest micro-focus computed tomography based on an all-optical inverse Compton scattering source," Matter Radiat. Extremes **5**, 064401 (2020).

[6]W. Wang, K. Feng, L. Ke, C. Yu, Y. Xu, R. Qi, Y. Chen, Z. Qin, Z. Zhang, M. Fang, J. Liu, K. Jiang, H. Wang, C. Wang, X. Yang, F. Wu, Y. Leng, J. Liu, R. Li, and Z. Xu, "Free-electron lasing at 27 nanometres based on a laser wakefield accelerator," Nature **595**, 516–520 (2021).

[7]X.-L. Zhu, W.-Y. Liu, S.-M. Weng, M. Chen, Z.-M. Sheng, and J. Zhang, "Generation of single-cycle relativistic infrared pulses at wavelengths above 20 μm from density-tailored plasmas," Matter Radiat. Extremes **7**, 014403 (2022).

[8]W. P. Leemans, A. J. Gonsalves, H.-S. Mao, K. Nakamura, C. Benedetti, C. B. Schroeder, C. Tóth, J. Daniels, D. E. Mittelberger, S. S. Bulanov, J.-L. Vay, C. G. R. Geddes, and E. Esarey, "Multi-GeV electron beams from capillary-discharge-guided subpetawatt laser pulses in the self-trapping regime," Phys. Rev. Lett. **113**, 245002 (2014).

[9]A. J. Gonsalves, K. Nakamura, J. Daniels, C. Benedetti, C. Pieronek, T. C. H. de Raadt, S. Steinke, J. H. Bin, S. S. Bulanov, J. van Tilborg, C. G. R. Geddes, C. B. Schroeder, C. Tóth, E. Esarey, K. Swanson, L. Fan-Chiang, G. Bagdasarov, N. Bobrova, V. Gasilov, G. Korn, P. Sasorov, and W. P. Leemans, "Petawatt laser guiding and electron beam acceleration to 8 GeV in a laser-heated capillary discharge waveguide," Phys. Rev. Lett. **122**, 084801 (2019).

[10]A. Döpp, C. Thaury, E. Guillaume, F. Massimo, A. Lifschitz, I. Andriyash, J. P. Goddet, A. Tazfi, K. Ta Phuoc, and V. Malka, "Energy-chirp compensation in a laser wakefield accelerator," Phys. Rev. Lett. **121**, 074802 (2018).

[11]W. T. Wang, W. T. Li, J. S. Liu, Z. J. Zhang, R. Qi, C. H. Yu, J. Q. Liu, M. Fang, Z. Y. Qin, C. Wang, Y. Xu, F. X. Wu, Y. X. Leng, R. X. Li, and Z. Z. Xu, "High-brightness high-energy electron beams from a laser wakefield accelerator via energy chirp control," Phys. Rev. Lett. **117**, 124801 (2016).

[12]L. T. Ke, K. Feng, W. T. Wang, Z. Y. Qin, C. H. Yu, Y. Wu, Y. Chen, R. Qi, Z. J. Zhang, Y. Xu, X. J. Yang, Y. X. Leng, J. S. Liu, R. X. Li, and Z. Z. Xu, "Near-GeV electron beams at a few per-mille level from a laser wakefield accelerator via density-tailored plasma," Phys. Rev. Lett. **126**, 214801 (2021).

[13]W. P. Leemans, B. Nagler, A. J. Gonsalves, C. Toth, K. Nakamura, C. G. R. Geddes, E. Esarey, C. B. Schroeder, and S. M. Hooker, "GeV electron beams from a centimetre-scale accelerator," Nat. Phys. **2**, 696 (2006).

[14]A. Pak, K. A. Marsh, S. F. Martins, W. Lu, W. B. Mori, and C. Joshi, "Injection and trapping of tunnel-ionized electrons into laser-produced wakes," Phys. Rev. Lett. **104**, 025003 (2010).

[15]J. Vieira, S. F. Martins, V. B. Pathak, R. A. Fonseca, W. B. Mori, and L. O. Silva, "Magnetic control of particle injection in plasma based accelerators," Phys. Rev. Lett. **106**, 225001 (2011).

[16]A. Buck, J. Wenz, J. Xu, K. Khrennikov, K. Schmid, M. Heigoldt, J. M. Mikhailova, M. Geissler, B. Shen, F. Krausz, S. Karsch, and L. Veisz, "Shock-front injector for high-quality laser-plasma acceleration," Phys. Rev. Lett. **110**, 185006 (2013).

[17]D. Umstadter, J. K. Kim, and E. Dodd, "Laser injection of ultrashort electron pulses into wakefield plasma waves," Phys. Rev. Lett. **76**, 2073–2076 (1996).

[18]E. Esarey, R. F. Hubbard, W. P. Leemans, A. Ting, and P. Sprangle, "Electron injection into plasma wakefields by colliding laser pulses," Phys. Rev. Lett. **79**, 2682–2685 (1997).

[19]Z. M. Sheng, W. M. Wang, R. Trines, P. Norreys, M. Chen, and J. Zhang, "Mechanisms of electron injection into laser wakefields by a weak counter-propagating pulse," Eur. Phys. J.: Spec. Top. **175**, 49–55 (2009).

[20]J. Faure, C. Rechatin, A. Norlin, A. Lifschitz, Y. Glinec, and V. Malka, "Controlled injection and acceleration of electrons in plasma wakefields by colliding laser pulses," Nature **444**, 737–739 (2006).

[21]A. G. R. Thomas, C. D. Murphy, S. P. D. Mangles, A. E. Dangor, P. Foster, J. G. Gallacher, D. A. Jaroszynski, C. Kamperidis, K. L. Lancaster, P. A. Norreys, R. Viskup, K. Krushelnick, and Z. Najmudin, "Monoenergetic electronic beam production using dual collinear laser pulses," Phys. Rev. Lett. **100**, 255002 (2008).

[22]H. Kotaki, I. Daito, M. Kando, Y. Hayashi, K. Kawase, T. Kameshima, Y. Fukuda, T. Homma, J. Ma, L.-M. Chen, T. Z. Esirkepov, A. S. Pirozhkov, J. K. Koga, A. Faenov, T. Pikuz, H. Kiriyama, H. Okada, T. Shimomura, Y. Nakai, M. Tanoue, H. Sasao, D. Wakai, H. Matsuura, S. Kondo, S. Kanazawa, A. Sugiyama, H. Daido, and S. V. Bulanov, "Electron optical injection with head-on and countercrossing colliding laser pulses," Phys. Rev. Lett. **103**, 194803 (2009).

[23]C. Rechatin, J. Faure, A. Ben-Ismail, J. Lim, R. Fitour, A. Specka, H. Videau, A. Tafzi, F. Burgy, and V. Malka, "Controlling the phase-space volume of injected electrons in a laser-plasma accelerator," Phys. Rev. Lett. **102**, 164801 (2009).

[24]G. Golovin, W. Yan, J. Luo, C. Fruhling, D. Haden, B. Zhao, C. Liu, M. Chen, S. Chen, P. Zhang, S. Banerjee, and D. Umstadter, "Electron trapping from interactions between laser-driven relativistic plasma waves," Phys. Rev. Lett. **121**, 104801 (2018).

[25]Q. Chen, D. Maslarova, J. Wang, S. X. Lee, V. Horný, and D. Umstadter, "Transient relativistic plasma grating to tailor high-power laser fields, wakefield plasma waves, and electron injection," Phys. Rev. Lett. **128**, 164801 (2022).

[26]X. Davoine, E. Lefebvre, C. Rechatin, J. Faure, and V. Malka, "Cold optical injection producing monoenergetic, multi-GeV electron bunches," Phys. Rev. Lett. **102**, 065001 (2009).

[27]R. Lehe, A. F. Lifschitz, X. Davoine, C. Thaury, and V. Malka, "Optical transverse injection in laser-plasma acceleration," Phys. Rev. Lett. **111**, 085005 (2013).

[28]R. Hu, H. Lu, Y. Shou, C. Lin, H. Zhuo, C.-e. Chen, and X. Yan, "Brilliant GeV electron beam with narrow energy spread generated by a laser plasma accelerator," Phys. Rev. Accel. Beams **19**, 091301 (2016).

[29]M. Zeng, A. M. de la Ossa, and J. Osterhoff, "Ponderomotively assisted ionization injection in plasma wakefield accelerators," New J. Phys. **22**, 123003 (2020).

[30]J. Wang, M. Zeng, X. Wang, D. Li, and J. Gao, "Scissor-cross ionization injection in laser wakefield accelerators," Plasma Phys. Controlled Fusion **64**, 045012 (2022).
[31]G. Wittig, O. Karger, A. Knetsch, Y. Xi, A. Deng, J. B. Rosenzweig, D. L. Bruhwiler, J. Smith, G. G. Manahan, Z.-M. Sheng, D. A. Jaroszynski, and B. Hidding, "Optical plasma torch electron bunch generation in plasma wakefield accelerators," Phys. Rev. Spec. Top.–Accel. Beams **18**, 081304 (2015).
[32]L.-L. Yu, E. Esarey, C. B. Schroeder, J.-L. Vay, C. Benedetti, C. G. R. Geddes, M. Chen, and W. P. Leemans, "Two-color laser-ionization injection," Phys. Rev. Lett. **112**, 125001 (2014).
[33]B. Hidding, G. Pretzler, J. B. Rosenzweig, T. Königstein, D. Schiller, and D. L. Bruhwiler, "Ultracold electron bunch generation via plasma photocathode emission and acceleration in a beam-driven plasma blowout," Phys. Rev. Lett. **108**, 035001 (2012).
[34]N. Bourgeois, J. Cowley, and S. M. Hooker, "Two-pulse ionization injection into quasilinear laser wakefields," Phys. Rev. Lett. **111**, 155004 (2013).
[35]D. Maslarova, M. Krus, V. Horny, and J. Psikal, "Laser wakefield accelerator driven by the super-Gaussian laser beam in the focus," Plasma Phys. Controlled Fusion **62**, 024005 (2020).
[36]P. Mora and T. M. Antonsen, Jr., "Kinetic modeling of intense, short laser pulses propagating in tenuous plasmas," Phys. Plasmas **4**, 217–229 (1997).
[37]A. Martinez de la Ossa, Z. Hu, M. J. V. Streeter, T. J. Mehrling, O. Kononenko, B. Sheeran, and J. Osterhoff, "Optimizing density down-ramp injection for beam-driven plasma wakefield accelerators," Phys. Rev. Accel. Beams **20**, 091301 (2017).
[38]X. L. Xu, F. Li, W. An, T. N. Dalichaouch, P. Yu, W. Lu, C. Joshi, and W. B. Mori, "High quality electron bunch generation using a longitudinal density-tailored plasma-based accelerator in the three-dimensional blowout regime," Phys. Rev. Accel. Beams **20**, 111303 (2017).
[39]R. Lehe, M. Kirchen, I. A. Andriyash, B. B. Godfrey, and J.-L. Vay, "A spectral, quasi-cylindrical and dispersion-free particle-in-cell algorithm," Comput. Phys. Commun. **203**, 66–82 (2016).
[40]J.-L. Vay, A. Huebl, A. Almgren, L. D. Amorim, J. Bell, L. Fedeli, L. Ge, K. Gott, D. P. Grote, M. Hogan, R. Jambunathan, R. Lehe, A. Myers, C. Ng, M. Rowan, O. Shapoval, M. Thévenet, H. Vincenti, E. Yang, N. Zaïm, W. Zhang, Y. Zhao, and E. Zoni, "Modeling of a chain of three plasma accelerator stages with the WarpX electromagnetic PIC code on GPUs," Phys. Plasmas **28**, 023105 (2021).
[41]W. Lu, M. Tzoufras, C. Joshi, F. S. Tsung, W. B. Mori, J. Vieira, R. A. Fonseca, and L. O. Silva, "Generating multi-GeV electron bunches using single stage laser wakefield acceleration in a 3D nonlinear regime," Phys. Rev. Spec. Top.–Accel. Beams **10**, 061301 (2007).
[42]M. Zeng, M. Chen, Z.-M. Sheng, W. B. Mori, and J. Zhang, "Self-truncated ionization injection and consequent monoenergetic electron bunches in laser wakefield acceleration," Phys. Plasmas **21**, 030701 (2014).